# Correction to the Schenk Model of Band-to-Band Tunneling in Silicon Applied to the Simulation of Nanowire Tunneling Transistors

Alexander Heigl*, Andreas Schenk† and Gerhard Wachutka*
*Institute for Physics of Electrotechnology, TU München, Arcisstrasse 21, 80333 München, Germany
Email: heigl@tep.ei.tum.de
†Integrated Systems Laboratory, Swiss Federal Institute of Technology, Gloriastrasse 35, 8092 Zürich, Switzerland

***Abstract*—We found out that the standard form of Schenk's model of band-to-band tunneling in silicon [1] involves a poor approximation of the Airy-Integral and, therefore, overestimates the channel currents of realistic tunneling devices. In this paper we propose a better approximation resulting in a corrected form of the model, and we demonstrate its impact on the device characteristics of a tunneling transistor. Additionally, we investigated the influence of the corrected model on the local density correction and quantum confinement.**

## I. Introduction

In modern nanometer MOS-devices band-to-band tunneling in silicon is of great importance: The progressive shrinking of the physical gate length of MOS-devices lead to undesired shortchannel effects such as drain-induced barrier lowering or punch-through. To some extent these can be reduced and in many cases even avoided by scaling the vertical dimensions of the devices. But nevertheless a number of problems are still remaining, in particular the leakage currents caused by parasitic tunneling. Examples are gate-induced drain leakage (GIDL) or direct tunneling through the gate oxide. This GIDL as a band-to-band tunneling effect is directly caused by the downscaling, since higher doping concentrations and steeper gradients are neccessary for smaller devices. An alternative approach to tackling short channel effects relies on device concepts such as the tunneling field effect transistor [2]. The primary working principle of this device is gate-controlled band-to-band tunneling through a $p^+n$-junction.

In the following section we briefly sketch the properties of the band-to-band tunneling model of Schenk. Afterwards we analyze the approximation error in the original model and present how the correct series expansion of the Airy-Integral is affecting the model. Since the complete model is depending on a sum of different types of Airy-Functions and Integrals we present an alternative to obtain a better suited approximation. Finally, we present elaborate investigations on the application of the corrected model to the simulation of cylindrical nanowire tunneling transistors.

## II. Modelling band-to-band tunneling

Phonon-assisted band-to-band tunneling is modeled on the basis of the Kubo formalism for the tunneling conductivity. For that purpose the constant field approximation is used, where

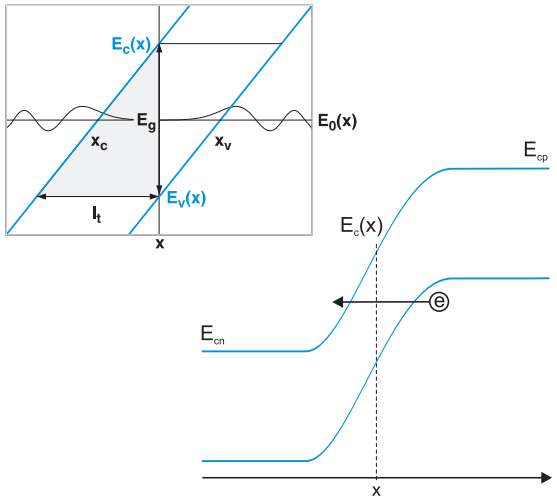


Fig. 1. Energy band diagramm and band-to-band tunneling region where a constant electric field is assumed [1].

the electric field is assumed to be constant over the complete tunneling length $l_t$ (see Fig. 1). With the phonon occupation number $f_B$ and the electric field $F$ this results in an equivalent recombination rate of the form

$$R^{bbt} = A \cdot F^2 \cdot D \cdot \left[ f_B H(x^{\mp}) + (f_B + 1)\, H(x^{\pm}) \right] \qquad (1)$$

where $x^{\pm}$ depends on the the electric field and the indirect energy band-gap [1], and the lower and upper sign describe tunneling under forward and reverse bias, respectively. One obtains

$$x^{\pm} = \left( \frac{3}{2} \frac{F_c^{\pm}}{F} \right)^{2/3} \qquad (2)$$

with the critical field strength $F_c^{\pm} \approx 2.5 \cdot 10^7$ V/cm. Since the field strenght in the devices of interest stays well below a few $10^6$ V/cm the values of $x^{\pm}$ are larger than five. $D$ denotes the difference of the Fermi-Dirac distribution functions

$$D = f_v - f_c = \frac{n_i^2 - np}{(n + n_i) \cdot (p + n_i)} \qquad (3)$$

The function $H(x)$ is the short notation of

$$H(x) = \frac{Ai(x)}{x^2} + \frac{Ai'(x)}{x} + Ai_1(x) \qquad (4)$$

978-1-4244-3927-0/09/$25.00 ©2009 IEEE

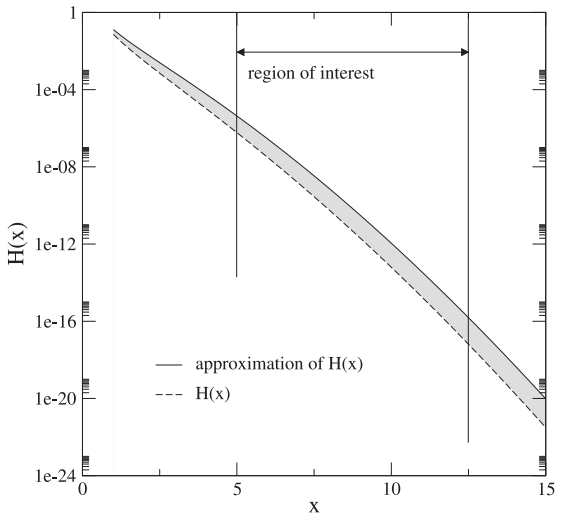


Fig. 2. Exact plot of $H(x)$ and the approximation of H(x) used by Schenk (cf. equation (6)).

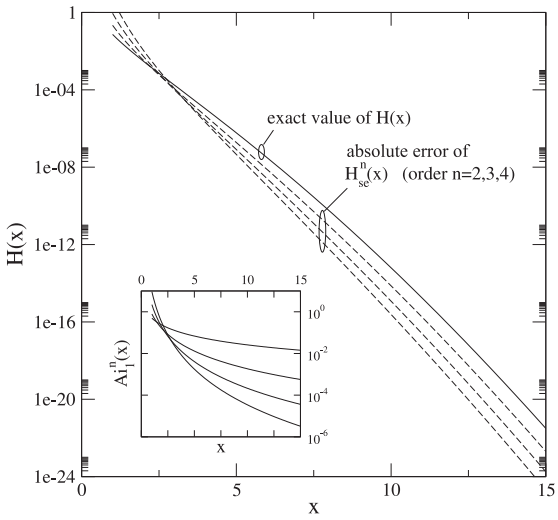


Fig. 3. Relative error of the series expansions of the Airy-integral $Ai_1(x)$ and absolute error of the resulting approximations of $H(x)$ in equation (9).

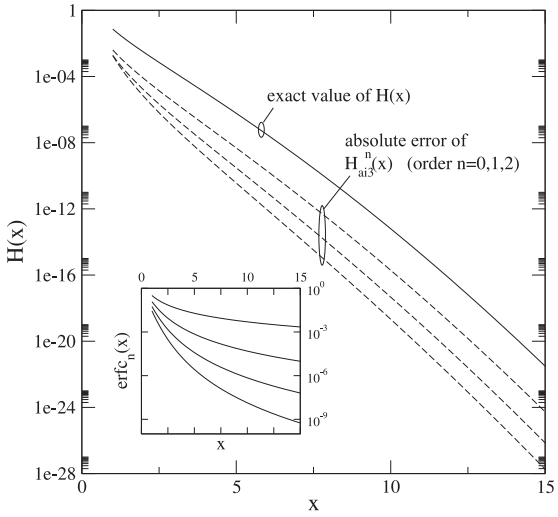


Fig. 4. Relative error of the approximations of the error-function and absolute error of approximations $H^n_{ai3}(x)$.

where $Ai(x)$ is the Airy function, $Ai'(x)$ its derivative with respect to $x$ and $Ai_1(x)$ the Airy-Integral, which is defined by

$$Ai_1(x) = \int_x^\infty Ai(y)dy \tag{5}$$

In his original paper Schenk used the approximation

$$H(x) \approx \frac{x^{-9/4}}{2\sqrt{\pi}} \cdot \exp\left(-\frac{2}{3}x^{3/2}\right) \qquad \text{for } x \to \infty \tag{6}$$

As demonstrated in Fig. 2, this is wrong by more than one order of magnitude. It should be noted, that for $x^\pm > 15$ the resulting generation/recombination rates are too low to be of any importance.

## III. Approximation of the Airy-Integral

Following the work of Nikishov and Ritus [3] one obtains the asymptotic series expansion of the Airy-Integral

$$Ai_1^n(x) = \frac{x^{-3/4}}{2\sqrt{\pi}} \exp\left(-\frac{2}{3}x^{3/2}\right) \cdot \sum_{i=0}^{n} a_i \cdot \left(-x^{-3/2}\right)^i \tag{7}$$

with the coefficients

$$a_0 = 1, \quad a_1 = \frac{41}{48}, \quad a_2 = \frac{9241}{4608}, \quad \ldots \tag{8}$$

The insert in Fig. 3 reveals the excellent approximation of the Airy-Integral. Using equation (7) for the calculation of $H(x)$ results in the following series expansion

$$H_{se}^n(x) = \frac{x^{-3/4}}{\sqrt{\pi}} \exp\left(-\frac{2}{3}x^{3/2}\right) \cdot \sum_{i=0}^{n} b_i \cdot \left(-x^{-3/2}\right)^i \tag{9}$$

with the coefficients

$$b_0 = 0, \quad b_1 = 0, \quad b_2 = 1, \quad b_3 = \frac{185}{48}, \quad \ldots \tag{10}$$

It should be noted that the first nonvanishing expression $H_{se}^2(x)$ is proportional to $x^{-15/4}$ which is in sharp contrast to the original approximation. In Fig. 3 the absolute errors of equation (9) are shown and one can observe the pretty high quality of these approximations in the region of interest. But nevertheless even for high orders the series $H_{se}^n(x)$ has large errors at small values of $x$.

To obtain better results we use the identity (26) of [3]

$$H(x) = 2\int_x^\infty \frac{Ai(y)}{y^3}dy \tag{11}$$

and insert the series expansion of the Airy-Function. In Fig. 4 the resulting approximations $H_{ai3}^n(x)$ are depicted. Since these expressions contain the error-function we use a continuous fraction as approximation (see insert in Fig. 4):

$$\text{erfc}(x) \approx \text{erfc}_2(x) = \frac{\exp(-x^2)}{\sqrt{\pi}\left(x + \frac{1}{2x+2/x}\right)} \tag{12}$$

Using this expression and the first element of the series

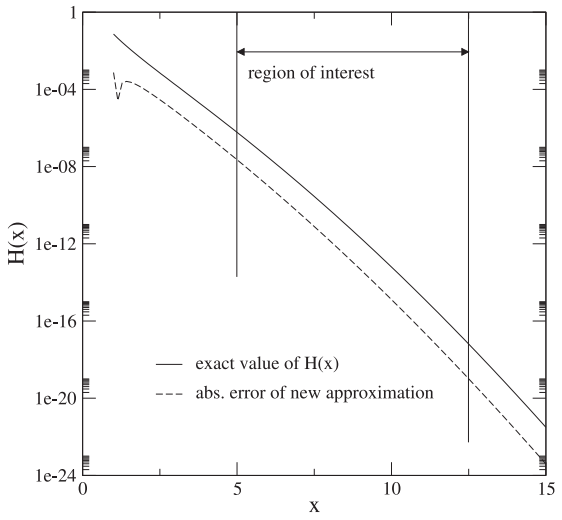


Fig. 5. Exact plot of $H(x)$ and absolute error of the corrected approximation used in equation (14).

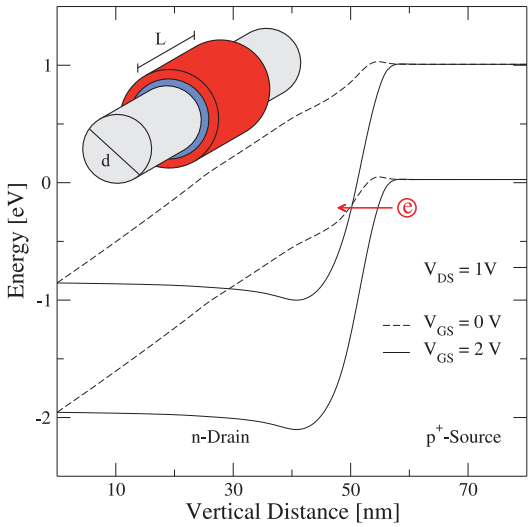


Fig. 6. Band diagram and structure of the cylindrical nanowire tunneling transistor at $V_{DS} = 1\,V$.

expansion of $Ai(x)$ in equation (11) we obtain after integration

$$H_0^2(x) = \frac{1}{\sqrt{\pi}} \cdot \frac{x^{-9/4}}{x^{3/2} + 9/4} \cdot \exp\left(-\frac{2}{3}x^{3/2}\right) \qquad (13)$$

A further numerical optimization of this approximation results in our proposed model correction

$$H(x) \approx \frac{1}{\sqrt{\pi}} \cdot \frac{x^{-9/4}}{x^{3/2} + 3} \cdot \exp\left(-\frac{2}{3}x^{3/2}\right) \qquad (14)$$

which has an absolute error that is nearly two orders of magnitude smaller than the values of $H(x)$ (see Fig. 5). In contrast to the original Schenk model the dependence of the recombination rate on the electric field is now $R^{bbt} \sim F^{9/2}$ (instead of $R^{bbt} \sim F^{7/2}$).

## IV. Simulation Results

Our simulations have been performed using the device simulator SENTAURUS. We studied a cylindrical nanowire tunneling transistor of 10 nm gate length and 15 nm diameter (see insert in Fig. 6). The transistor is built by a $10^{17}\,\mathrm{cm}^{-3}$ arsenic-doped drain region and a $5 \cdot 10^{19}\,\mathrm{cm}^{-3}$ boron-doped source region. The slope of the source doping profile is as steep as 2 nm/dec, and the gate is formed by a 2 nm $SiO_2$ layer and a TiN metallization. The resulting position-dependent energy band diagram calculated along a cutline parallel to the cylinder axis in a depth of 1 nm underneath the gate oxide for varying gate voltage clearly demonstrates the formation of the tunneling region (see Fig. 6).

Due to quantum confinement effects the electron density underneath the gate oxide is in reality very different from the one obtained by a pure classical treatment. Such quantum confinement effects must be properly included in the device simulation tools. But in many situations a quantum-mechanical treatment in terms of the solution of a Schrödinger-Poisson system is computationally prohibitive. Alternatively, the quasi-classical treatment of nanometer devices can be justified by

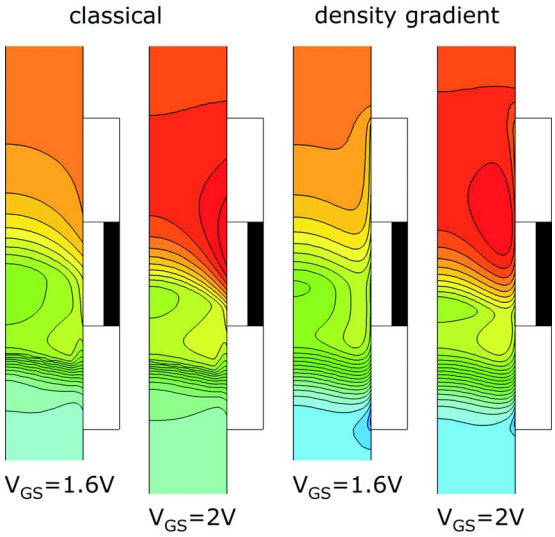


Fig. 7. Influence of quantum confinement on the electron density under the gates in a cylindrical nanowire TFET.

introducing a quantum-potential as correction of the Fermi levels. The density gradient model is based on the assumption that Bohm's potential [4] may be written as

$$\Lambda = -\frac{\gamma\hbar^2}{6m^\star\sqrt{n}}\nabla^2\sqrt{n} \qquad (15)$$

where the empirical parameter $\gamma$ accounts for the relative occupancy of the different subbands. The electron density is given by the Fermi-Dirac distribution where $\Lambda$ is incorporated as correction. Combining both expressions results in an equation for the quantum-potential which has to be solved together with Poissons equation and the carrier transport equations.

Fig. 7 depicts the influence of quantum confinement on the electron density under the gates in a cylindrical nanowire tunneling transistor. In addition, the results of a classical

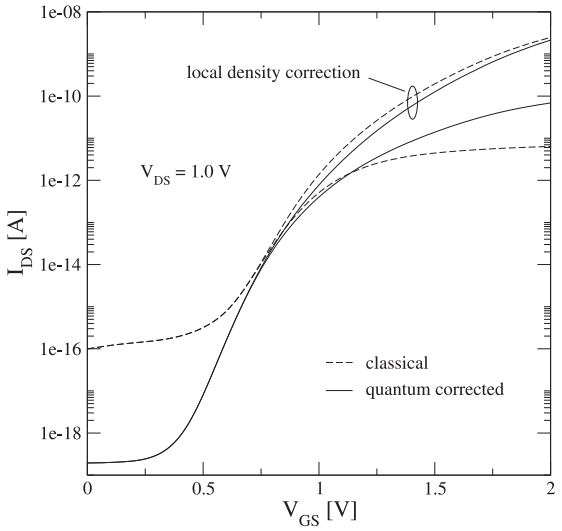


Fig. 8. Transfer characteristics of TFET with and w/o density gradient approach and local density correction.

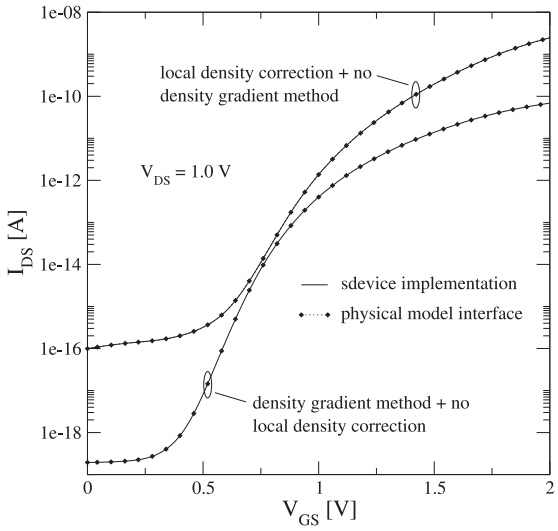


Fig. 9. Transfer characteristics as obtained from the physical model interface of Synopsys in comparison to the Sdevice implementation.

simulation are shown which confirm the expected the large difference between the two approaches. The maximum of the quantum-corrected electron density is separated from the $Si/SiO_2$ interface in a distance of about 1 nm.

Fig. 8 displays the simulated transfer characteristics of this cylindrical nanowire TFET for different model options: Since the tunneling current is dependent on the local values of the charge densities, one expects that the source-drain current will be quite sensitive to quantum mechanical corrections such as the density gradient potential, and this is clearly confirmed. The implemented model is local and, therefore, one observes an unphysical saturation of the tunneling rates for strong electric fields. This erroneous feature vanishes using the following local density correction

$$\widetilde{n} = n \cdot \left( \frac{n_i}{N_C} \right)^{\frac{\gamma_n \left| \nabla E_{f_n} \right|}{F}} \tag{16}$$

for the electrons (and a similar expression for the holes). The resulting transfer characteristics of this TFET reveal a very low blocking current and an excellent on-to-off current-relation.

In order to assess the impact of the corrected model on the transfer characteristics it is neccessary to rebuild the standard Schenk model via the physical model interface of Sentaurus device. Fig. 9 shows that this approach yields exactly the same results as the built-in model, and Fig. 10 reveals that the current through the nanowire tunneling transistor is significantly lowered by the corrected form of Schenk's model.

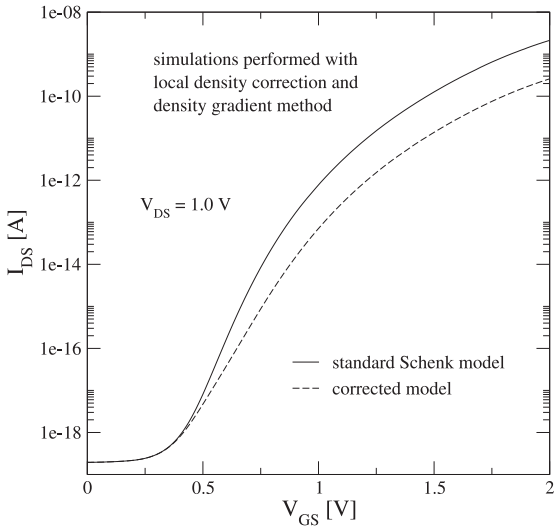


Fig. 10. Characteristics obtained from the corrected Schenk model compared to that from the standard form.

## V. Conclusions

We recognized that Schenk's model of band-to-band tunneling in silicon relies on a poor approximation of the Airy integral and, therefore, leads to inacceptable inaccuracies in the computed current densities. We propose a better approximation of the function $H(x)$, which however, results in a significant reduction of the equivalent generation rate. Furthermore, we implemented both models through the physical model interface in the device simulator Sentaurus Device and demonstrated the impact of the error correction on the simulation results of a cylindrical nanowire tunneling transistor.

## References


[1] A. Schenk, *Rigorous theory and simplified model of the band-to-band tunneling in silicon*, Solid State Electronics, **36**(1), pp. 19-34 (1993).

[2] W. Hansch, C. Fink, J. Schulze and I. Eisele, *A vertical MOS-gated Esaki tunneling transistor in silicon*, Thin Solid Films 369, 2000, pp.387-389.

[3] A.I. Nikishov, V.I. Ritus, *Asymptotic representations for some functions and integrals connected with the Airy function*, arXiv:math-ph/0501062v1 (2005).

[4] D. Bohm, *A suggested interpretation of the quantum theory in terms of hidden variables I and II*, Phys. Rev. 85(2), 1952, pp.166-193.

[5] A. Heigl, G. Wachutka, *Study on the optimized design of nanowire tunneling transistors including quantum effects*, Proceedings of SISPAD, pp. 225-228 (2008).

[6] *Sentaurus Device User Guide*, Synopsys Inc. (2007).